Pediatric Cardiology (2022) 43:1471–1480
https://doi.org/10.1007/s00246-022-02870-8

ORIGINAL ARTICLE

The Secrets of the Frogs Heart

Antonio F. Corno[1] · Zhen Zhou[2] · Santosh C. Uppu[1] · Shuning Huang[3] · Bruno Marino[4] · Dianna M. Milewicz[2] · Jorge D. Salazar[1]

Received: 11 February 2022 / Accepted: 4 March 2022 / Published online: 15 March 2022

Abstract

The heart of the African clawed frog has a double-inlet and single-outlet ventricle supporting systemic and pulmonary circulations via a truncus, and a lifespan of 25–30 years. We sought to understand the unique cardiac anatomic and physiologic characteristics, with balanced circulation and low metabolic rate, by comparing the basic anatomy structures with focused echocardiography and cardiac magnetic resonance imaging. Twenty-four adult female African clawed frogs were randomly subjected to anatomic dissection ($n=4$), echocardiography ($n=10$), and cardiac magnetic resonance ($n=10$). All anatomical features were confirmed and compared with echocardiography and cardiac magnetic resonance imaging. The main characteristics of the cardiovascular circulation in frogs are the following: Intact interatrial septum, with two separate atrio-ventricular valves, preventing atrial mixing of oxygenated and desaturated blood. Single spongiform ventricular cavity, non-conducive for homogeneous mixing. Single outlet with a valve-like mobile spiral structure, actively streaming into systemic and pulmonary arteries. Intact interatrial septum, spongiform ventricle, and valve-like spiral in the conus arteriosus are likely responsible for balanced systemic and pulmonary circulation in frogs, in spite of double-inlet and single-outlet ventricle.

Keywords Congenital heart defects · Heart · Single ventricle · Truncus arteriosus · *Xenopus Laevis*

Introduction

Xenopus Laevis (African clawed frog) have a single ventricle sustaining the systemic and pulmonary circulations, similar to 15% of children with complex congenital heart defects with "functionally" single ventricle. The long-term outcomes of patients with "functionally" uni-ventricular hearts are complicated by the combination of heart failure and cyanosis, substantially reducing their life expectancy and severely compromising their quality of life [1–11]. Reports of patients born with single ventricle, surviving to the adult life without any surgical treatment, are exceptionally rare [1, 12–14]. Children born with a "functionally" uni-ventricular heart generally require at least 2–3 staged operations to make the single ventricle pump the oxygenated blood to the systemic circulation, while the desaturated blood flows passively from the superior and inferior vena cava directly through the lungs [1–3]. This artificial circulation causes high systemic venous pressure, and the chronic elevation of the systemic venous pressure may results in liver failure, renal failure, protein-losing enteropathy, and plastic bronchitis [4–11].

Mathematical and computational fluid dynamic models were used to study the blood flow distribution in single ventricle, and to study and plan for a better type of circulation after Fontan procedure, altering traditional surgical options to possibly improve the efficiency of blood circulation and clinical outcomes [15–18]. Unfortunately, the limits intrinsic to all the theoretical models do not allow the simultaneous

Antonio F. Corno and Zhen Zhou: Equally contributing first authors

✉ Antonio F. Corno
antonio.f.corno@uth.tmc.edu

1 Children's Heart Institute, Memorial Hermann Children's Hospital, McGovern Medical School, University of Texas Health, 6431 Fannin Street, MSB 6.274, Houston, TX 77030, USA

2 Medical Genetics, Department of Internal Medicine, McGovern Medical School, University of Texas Health, Houston, TX 77030, USA

3 Department of Diagnostic and Interventional Imaging, McGovern Medical School, University of Texas Health, Houston, TX 77030, USA

4 Department of Pediatrics, Obstetrics and Gynecology, University La Sapienza, 00161 Roma, Italy

introduction of all the biological variables present in living individuals. In particular, the interference and interaction occurring due to the change of any biological parameters cannot be included.

Research on "functionally" uni-ventricular hearts would greatly benefit from studies performed on animals born with single ventricle, but the only animal models available in nature are amphibians, like *Xenopus Laevis*, and reptiles [19]. The *Xenopus Laevis* heart has a single ventricular chamber receiving the oxygenated blood coming from the lungs and draining into the left atrium, and the less saturated blood returning from the body and draining into the right atrium. The heart distributes the blood back to the pulmonary and systemic circulations through a single ventricular outlet, the conus arteriosus, that divides into right and left truncus arteriosus, each one with the lateral branch for the lung and skin perfusion, the medial one for the body perfusion, and the central one for the perfusion of the head [20–23].

Previous morphological studies, published more than fifty years ago, have investigated the peculiar anatomy of the frog's heart and tried to speculate on the cardiovascular function based on the morphology [24–26], but only recently those observations were correlated with the pathophysiology of the human hearts with single ventricle [27, 28].

In the *Xenopus Laevis* the gas exchanges occur through three different mechanisms: cutaneous, bucco-pharyngeal, and pulmonary respiration [23]. The cutaneous respiration takes place all the time, whether the frog is in or out of water; and when the frog is under water or hibernating, this is the only mode of respiration. The bucco-pharyngeal respiration is used on land, with the mouth permanently closed and the nostrils open. Moist skin and the buccal cavity supplement the oxygen provided through the pulmonary respiration [23]. Furthermore; amphibians have a substantially lower metabolic rate than mammals, including humans, reflected in the lower requirements for oxygen transport and cardiac output [23].

Despite the compensations of oxygen supply provided by skin and mouth, the heart of the *Xenopus Laevis* remains a heart with single ventricle, as in children with complex congenital heart defects; nevertheless it has been extremely well accounted for, by decades of research in reptiles and amphibians, that the *Xenopus* live a normal life for up to 25–30 years.

While studies have been published on the electrophysiology of the *Xenopus Laevis* heart [29–31], very little has been reported on the heart anatomy investigated by echocardiography [32], and, to the best of our knowledge, detailed information on the cardiovascular morphology investigated with microscopic dissecting techniques, as well as the anatomic correlations with echocardiography and cardiac magnetic resonance (CMR), have not yet been reported.

The purpose of our study was to investigate the cardiovascular anatomy of the *Xenopus Laevis* with microscopic dissecting techniques, echocardiography, and cardiac MRI.

Materials and Methods

Femal *Xenopus laevis* frogs purchased from NASCO (LM00531MX), were housed in the Center for Laboratory Animal Medicine and Care at The University of Texas Health Science Center at Houston (UTHealth) McGovern Medical School. All experiments were approved by the UTHealth Institutional Animal Care and Use Committee, Animal Welfare Committee, (protocol # AWC-19-0081). All *Xenopus Laevis* were housed in polycarbonate tanks on a recirculating system at a temperature of 16–19 °C, pH of 7.3–7.8, conductivity of 800–1500 µS/cm, and on a 12:12 light:dark cycle. Animals were fed frog brittle for Xenopus Laevis (SA05961 LM), NASCO) at twice/weekly intervals.

Anatomical Study

These four *Xenopus Laevis* (approximately 7 years of age) were obtained from an embryo research project from which they had been retired, due to declining egg quality and production.

General Anesthesia

General anesthesia was induced by immersion in 0.05% Benzocaine solution (neutralized ethyl 3-aminobenzoate methanesulfonate (= MS222, Sigma Aldrich, St. Louis, Missouri), buffered with sodium bicarbonate to pH 7-7.4, for 45 minutes. After checking for areflexia and for proper depth of anesthesia, the *Xenopus Laevis* were sacrificed by double-pithing technique with a 16G needle. The four *Xenopus* were then stored in ice wrapped towel, soaked with 0.05% Benzocaine solution, in plastic bags maintained at 4°C until the moment of dissection.

Dissection

Dissection was performed using the microscope Leica A60 (Leica Biosystems, Pathology Laboratory Equipment), and photographs were taken with the microscope Nikon SMZ 745 T Digital Sight DS-Fi2, using the software NIS-Elements F 4.00.00 (Nikon Microscopy Instruments), using the images of the dissected anatomy for this report.

Echocardiographic and Magnetic Resonance Imaging Study

Twenty *Xenopus* were randomly assigned to either echocardiographic (n = 10) or CMR (n = 10) investigations. Before imaging investigations each Xenopus was weighed, and a photo taken for identification.

General Anesthesia

General anesthesia was induced by immersion of the *Xenopus Laevis* in 0.05% Benzocaine solution (neutralized ethyl 3-aminobenzoate methanesulfonate (= MS222, Sigma Aldrich), 1.5 gram in 1 Liter of system water buffered with sodium bicarbonate to a pH of 7.0-7.4.

For induction, *Xenopus Laevis* were placed in a small tank containing MS222 solution, in a position with the head raised and the nostrils above the water line. After checking for areflexia to verify the depth of general anesthesia, the Xenopus *Laevis* were wrapped in a paper towel, soaked in MS222 maintenance solution. Electrocardiography and respiratory rate leads were attached to the skin of the fore limbs for monitoring purposes. The *Xenopus Laevis* was then positioned in supine position for either echocardiography or CMR.

Echocardiography

After general anesthesia, frogs still wrapped in paper towels soaked in MS222 maintenance solution to maintain proper skin moistening and anesthesic depth, were placed supine on the animal handling platform. Echocardiography investigation was performed using Vevo 3100 imaging system, MX250, 15–30 MHz transducer (VisualSonics, Toronto, Canada), basic anatomical structures were obtained under B-model, vascular blood flow stream was captured with color Doppler. Cardiovascular images were obtained from the subcostal plane, sagittal plane (parasternal long-axis), and axial view (parasternal short-axis). No Doppler measurements or functional evaluations were taken for this study.

Cardiac Magnetic Resonance (CMR)

CMR was conducted with a 7.0 Tesla Bruker BioSpect CMR system (Bruker BioSpin, Billerica MA) equipped with a BGA 12 gradient and shim system (12 cm inner diameter and 440 mT/m maximum gradient strength). Heart rate of the frog was monitored with a physiological system (Small Animal Instruments, Inc., Stony Brook, NY). A volume coil transmit and surface coil receive setup was used for all the imaging acquisition. Axial and coronal T2-weighted black blood images were acquired using 2D RARE sequence (TR: 4500 ms, Effective TE: 17.5 ms, 200×200 μm^2 in-plane resolution, and 0.5 mm slice thickness). Cine bright blood imaging with retrospective gating was acquired with the following imaging parameter: TR = 7.85 ms, TE = 2.1 ms, 118×118 μm^2 in-plane resolution, and 0.5 mm slice thickness.

Recovery

Once the echocardiography or the CMR investigations were completed, the frogs were removed from the wrapping and placed in a solid-sided recovery tank with system water with the head elevated to ensure that the nostrils were above the water line. Frogs were returned to their home tank once they were able to swim around the recovery tank, and were checked 24 h later to verify normal recovery. Feeding was restarted after 24 h, and frogs were re-weighed after 48 h and then at monthly intervals.

Imaging

For the anatomical directions we used the terminology of anterior and posterior, rather than ventral and dorsal, because the images were taken with the animals in supine position, rather than prone as generally reported in amphibians studies [24–26], and because our readership are mostly interested in the potential correlation with human subjects.

Results

The macroscopic findings were analyzed following the sequential anatomy, as for congenital heart defects, starting from the systemic and pulmonary venous connections, through the intra-cardiac structures, to the systemic and pulmonary arterial vessels [33].

On microscopic dissection, echocardiography, and cardiac MRI, right superior vena cava, left superior vena cava, and inferior vena cava, joined in the sinus venosus, located in the posterior aspect of the heart, while right and left pulmonary veins drained in the pulmonary venous collector, located above the sinus venosus collecting the systemic venous drainage (Fig. 1).

Dissection of the postero-superior aspect of the heart showed left and right atrium, with intact atrial septum completely separating the two atrio-ventricular valves. Echocardiography and cardiac MRI confirmed all these findings (Fig. 2). The presence of intact atrial septum, documented in the microscopic dissection, echocardiography and cardiac MRI investigations of all animals ($n = 24$), and the complete separation of the two atrio-ventricular valves, confirms that in the frog's heart there is complete streaming of the

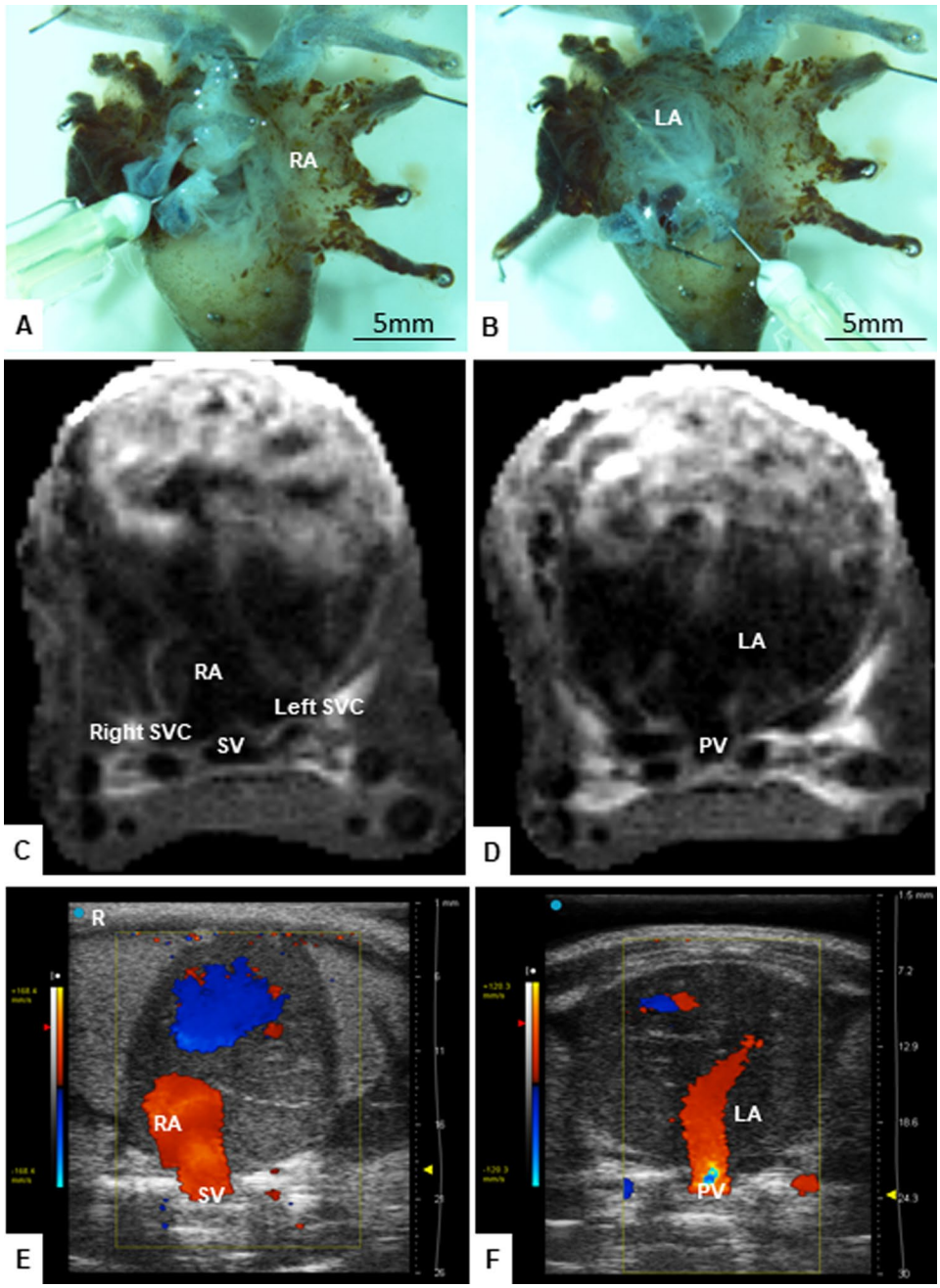

Fig. 1 Posterior aspect of the anatomical structures outside the pericardium of a *Xenopus* heart. **A** Right superior vena cava, left superior vena cava and inferior vena cava, joined in the sinus venosus, located in the posterior aspect of the heart; **B** Right and left pulmonary veins drained in the pulmonary venous collector, located above the sinus venosus collecting the systemic venous drainage; **C** and **D** MRI (black blood) axial view, and **E** and **F** color Doppler echocardiographic view of the sinus venosus draining in the right atrium, and of the pulmonary venous collector draining into the left atrium. *IVC* inferior vena cava, *LA* left atrium, *PV* pulmonary venous collector, *RA* right atrium, *SV* sinus venosus, *SVC* superior vena cava

oxygenated blood of the left atrium from the less saturated blood of the right atrium. In all frogs, echocardiography and cardiac MRI investigation were never able to show any evidence of stenosis of regurgitation of either of the two atrio-ventricular valves.

The anterior dissection of the single ventricular cavity confirmed the morphology of double-inlet single ventricle, with right and left atrium connected to the single ventricle by two atrio-ventricular valves completely separated by fibrous tissue, anchored in the atrial septum and the medial atrio-ventricular canal myocardium or first tract of the ventricular inlet (Fig. 3). This anatomical characteristic, typical of amphibians, maintains the streaming of the blood drained from the right and left atrium. The single ventricular cavity presents with a very spongiform and trabeculated structure, certainly non-conducive for homogeneous blood mixing. In addition, contrary to previous reports [34], we observed a fibrous continuity between the annulus of the right atrio-ventricular valve and the annulus of the truncal valve, which has three semilunar leaflets (Fig. 3). As a result, the less saturated blood coming from the right atrio-ventricular valve has a shorter pathway toward the initial segment of the conus arteriosus, where

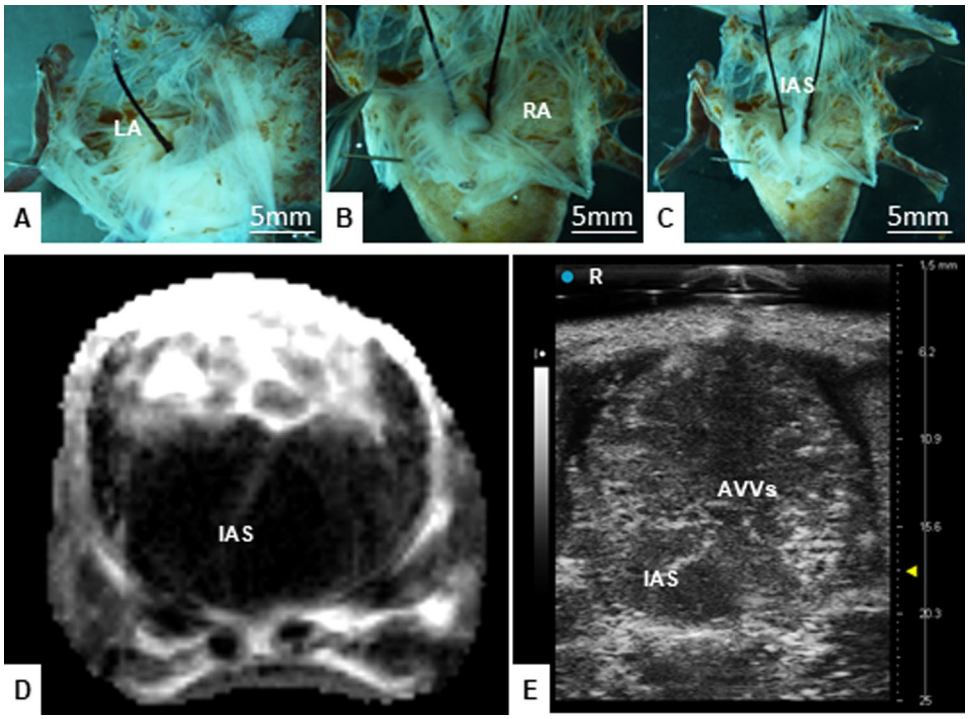

Fig. 2 Postero-superior aspect of right and left atrium in a *Xenopus* heart. **A** left atrium, with a suture probe through the left atrio-ventricular valve; **B** right atrium, with suture probes through the right and left atrio-ventricular valves; **C** left and right atrium, with suture probes through the right and left atrio-ventricular valves, and the spiral form of the intact atrial septum; **D** MRI (black blood) axial view, and **E** B-mode echo-cardiographic view, showing the intact atrial septum dividing the two atrio-ventricular valves. *AVVs* atrio-ventricular valves, *IAS* inter-atrial septum, *LA* left atrium, *RA* right atrium

the origins of the right and left pulmo-cutaneous branches are located.

The frontal view of the external appearance of the *Xenopus* heart showed the conus arteriosus originating from the supero-anterior right side of the single ventricular cavity, and immediately dividing in right and left branches (Fig. 4). The open dissection of the single ventricular outlet revealed the conus arteriosus, with a fibrous spiral structure located between the three semilunar leaflets of the truncal valve and the division of the conus in right and left truncus arteriosus (Fig. 4).

Microscopic dissection of the two branches of the truncus arteriosus showed their three arches: pulmo-cutaneous, systemic, and carotid branch, respectively, in lateral, intermediate, and median location (Fig. 5).

Discussion

The findings of our observations confirm some of the previously reported findings of the cardiovascular anatomy. The *Xenopus Laevis*, as the other amphibians, has a functionally uni-ventricular heart, with a single ventricular cavity receiving the oxygenated blood from the left atrium and the less saturated blood from the right atrium, with the atrial chambers in situs solitus. What was never reported, to the best of our knowledge, is the complete separation of the pulmonary and systemic venous returns by an intact inter-atrial septum, not allowing any mixing of the fully oxygen saturated pulmonary venous return with the less saturated systemic venous blood. The drainage occurs into the single ventricular cavity with complete streaming through two separate atrio-ventricular valves, and a fibrous structure persistent in the first tract of the ventricular inlet. On the contrary, a previous study reported the presence of a common atrioventricular valve [32].

The ventricular morphology of the frog is extremely complex, with a structure very spongiform and trabeculated, different from the mammalian heart with a well-defined cavity. The direct fibrous continuity of the right atrio-ventricular valve with the semilunar truncal valve, and the fact that the right atrium drains in the superior and anterior part of the single ventricle, suggest the presence of D-ventricular loop [33]. Furthermore, the morphology of the single ventricular cavity allows to speculate that, most probably, the complete streaming of fully oxygen saturated and desaturated venous blood entering into the single ventricle from a double inlet of the two separate atrioventricular valves, somehow persists, at least partially, due to the anatomic characteristics of the single ventricle, where complete mixing seems highly improbable. In particular, the less saturated blood coming from the right atrium through the right atrio-ventricular valve, draining in the superior and anterior due to the proximity of the semilunar truncal valve, has the easier access to the only outlet from the single ventricle.

Another characteristic of the single ventricle in *Xenopus Laevis* is the evident disproportionate ration between mass and volume, in favor of the first one. This relationship of relatively large mass for a small volume of blood could explain the efficiency of the peculiar *Xenopus*

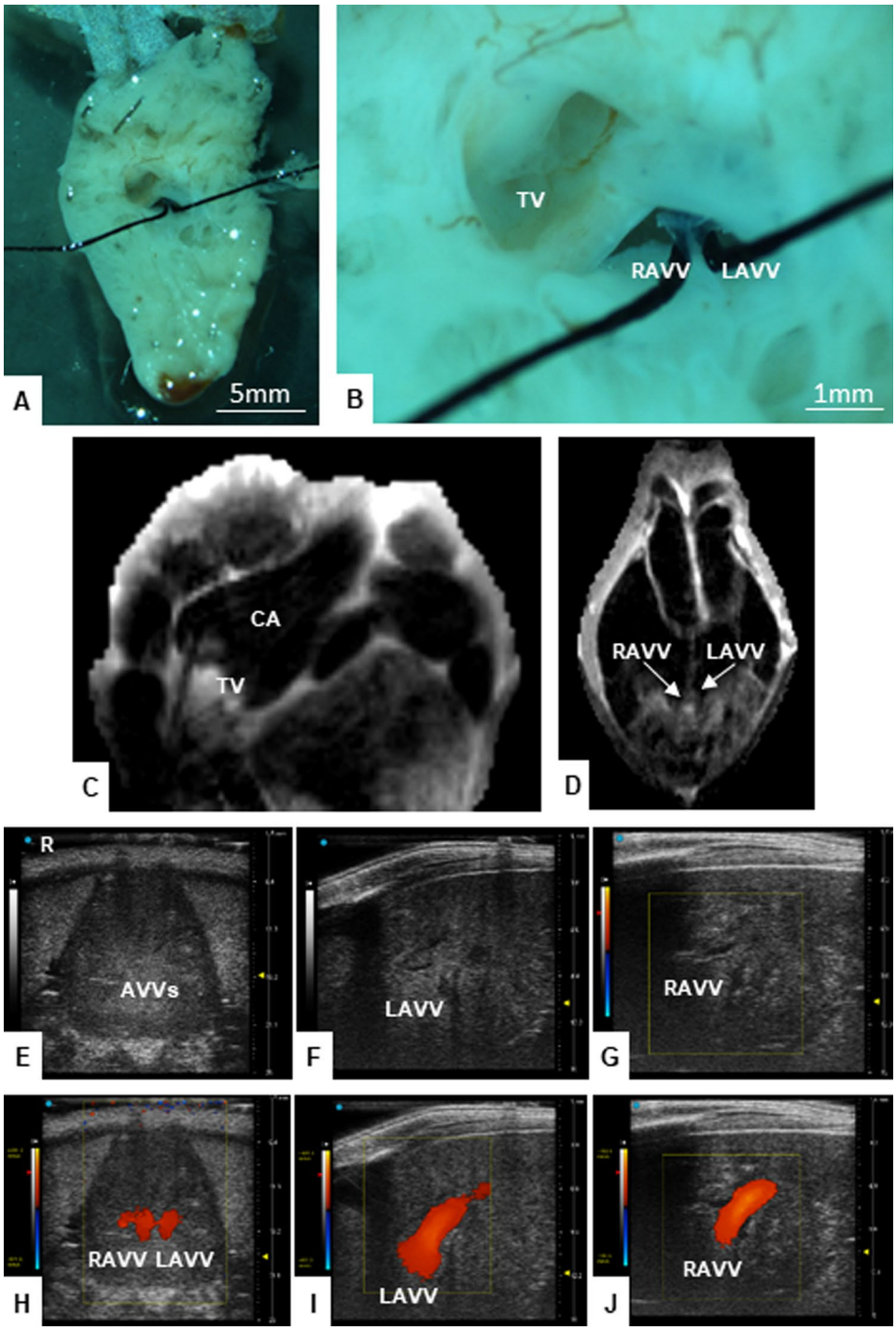

Fig. 3 Anterior dissection of the single ventricular cavity. Confirmation of the morphology of double-inlet single ventricle, with right and left atrium clearly connected to the single ventricle by two atrio-ventricular valves completely separated by fibrous tissue, even in the first tract of the ventricular inlet, as to maintain the blood streaming. The single ventricular cavity presents with of a very spongiform and trabeculated structure, with fibrous continuity between right atrio-ventricular valve and truncal valve annulus, which has three semilunar leaflets. **A** and **B** magnified, anatomical view; **C** and **D** MRI (black blood) coronal view, **E**, **F** and **G**, B-mode, and **H**, **I** and **J**, color Doppler echocardiographic view. *CA* conus arteriosus, *LAVV* left atrio-ventricular valve, *RAVV* right atrio-ventricular valve, *TV* truncal valve

myocardium, with a number of myofibrils adequate for a relatively reduced amount of work required to pump a relatively small volume of blood. An adequate cardiac output, and therefore oxygen delivery, is maintained with relatively low oxygen consumption, thanks to the good ventricular ejection fraction ($49.3 \pm 12.5\%$) and the low heart rate [32].

The single ventricular outlet is a conus arteriosus, divided in right and left truncus, each one with separate arteries for the perfusion of head, body and lungs.

The blood content of the ventricular cavity, presumably not completely mixed, encounters a further streaming in the outflow tract of the single ventricle, where a fibrous spiral structure, located between the semilunar leaflets of

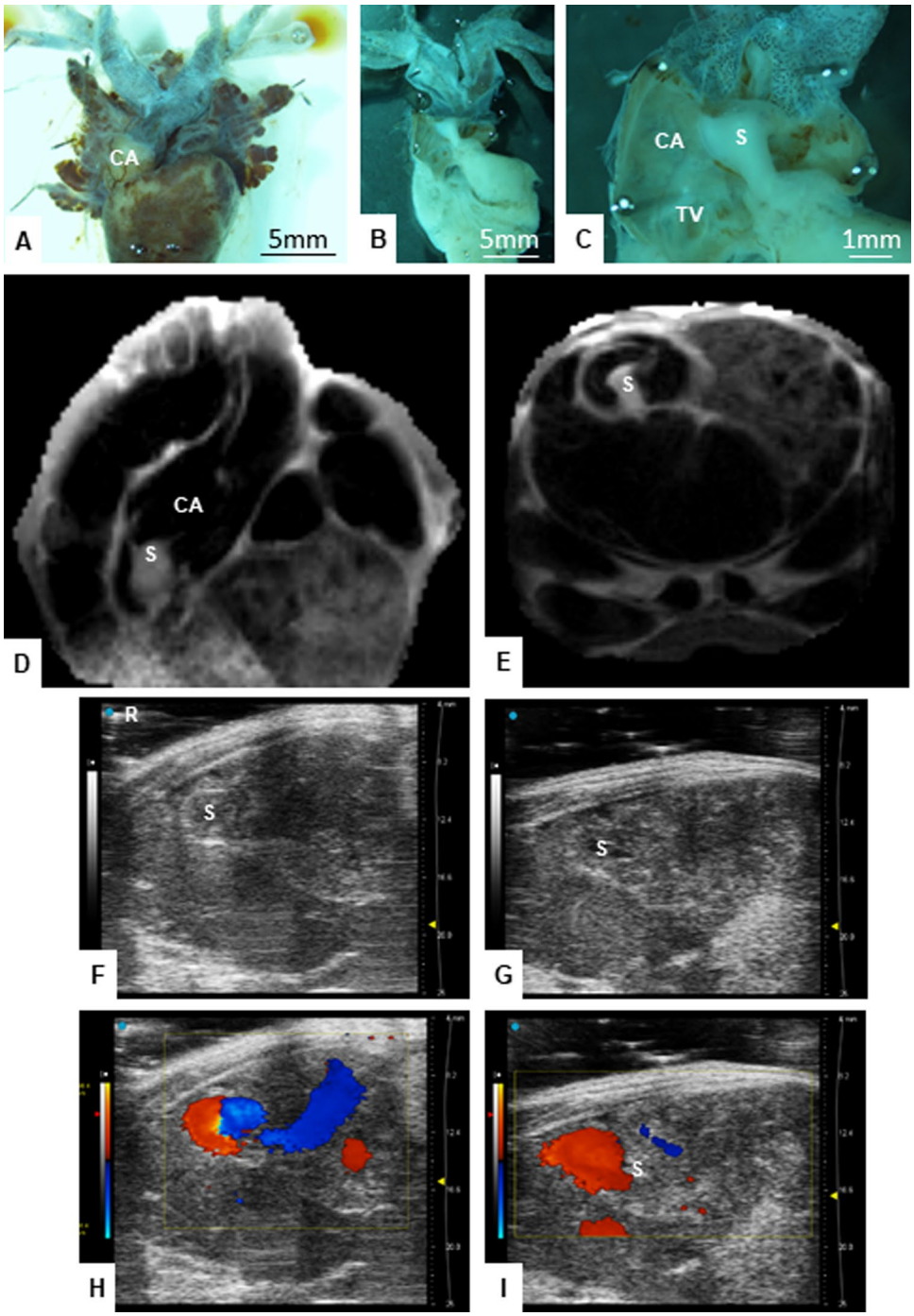

Fig. 4 Frontal view of the outflow tract from the single ventricle. **A** External appearance of the *Xenopus* heart, with the conus arteriosus originating from the supero-anterior right side of the single ventricular cavity, and immediately dividing in right and left branches; **B** Open dissection of the single outlet from the single ventricle revealing the conus arteriosus, with a fibrous spiral structure located between the three semilunar leaflets of the truncal valve and the division of the conus in right and left truncus arteriosus; **C** Same image, magnified. **D** MRI (black blood) coronal view, and **E** MRI (black blood) axial view, and **F** and **G** B-mode echocardiographic view, and **H** and **I** color Doppler echocardiographic view of the conus arteriosus with the spiral structure. *CA* conus arteriosus, *S* spiral, *TV* truncal valve

the truncal valve and the division of the conus in right and left truncus arteriosus, provides a separation of blood flows toward the truncal arteries.

The spiral pattern of the fibrous structure within the conus follows the same rightward direction (counter clock wise when seen from above) of the spiral rotation of the mammalian and human cardiac infundibula and great arteries, in relation with the Nodal gene pathway Ptx2 and Xnr-1 observed in *Xenopus Laevis* [35–38]. Not only is the Nodal gene well present in frogs, but it can be suggested that the similar cardiac phenotype and the genetic background represent an effect of the evolutionary development since the Nodal gene was documented to be the cause of the spiral pattern in shells and snails [39–41]. The Nodal signaling present in *Xenopus Laevis* supports the previously suggested biological link between the spiral pattern of the ventricular infundibula and great arteries, where multiple mutations of this laterality gene are responsible

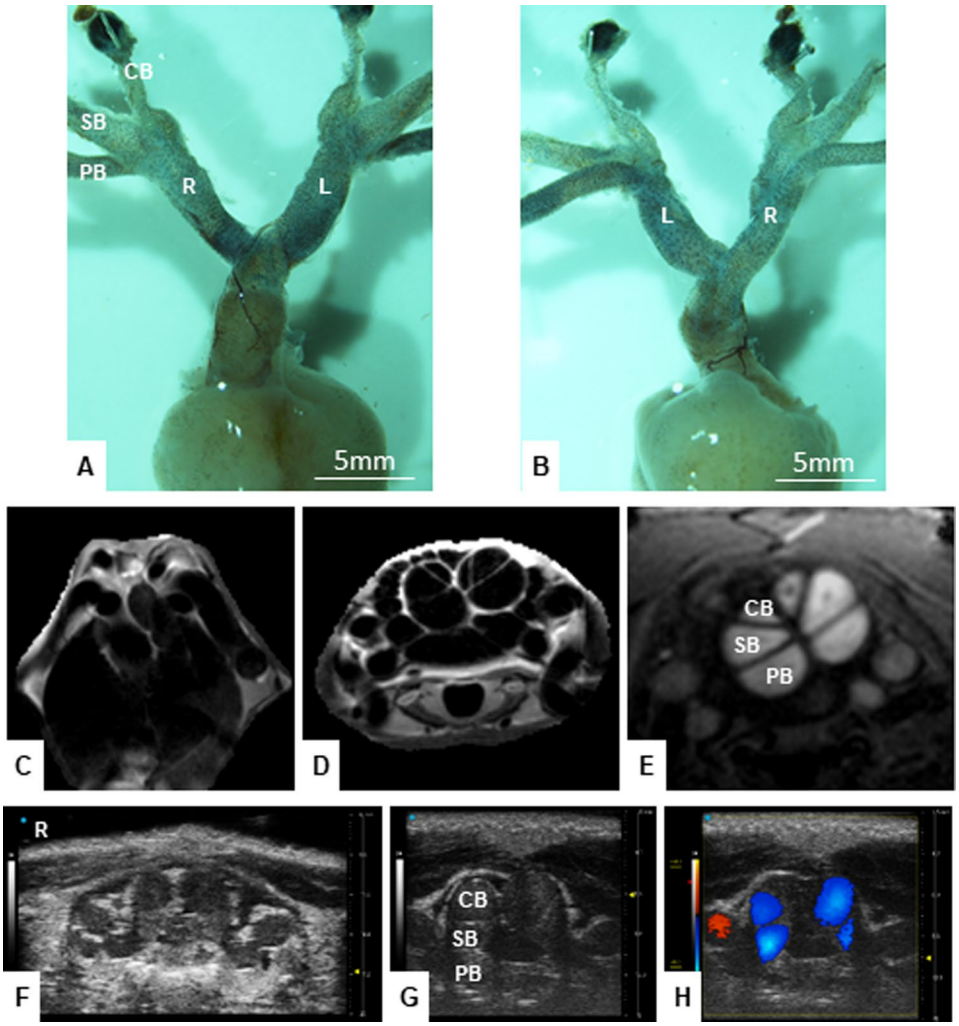

Fig. 5 **A** Anterior and **B** posterior aspects of the two branches of the truncus arteriosus and its three arches: pulmo-cutaneous, systemic, and carotid branch, respectively, in lateral, intermediate, and median location; **C** MRI (black blood) coronal view, and **D** MRI (black blood) axial view, and **E** MRI (white blood) axial view, **F** and **G** B-mode echocardiographic view, and **H** color Doppler echocardiographic view of the truncus arteriosus and its branches. *CB* carotid branch, *L* left, *PB* pulmo-cutaneous branch, *R* right, *SB* systemic branch

for the presence of complex trunco-conal congenital heart defects [42–44].

Our observations of the anatomical configuration confirm that the heart of frogs is not completely septated, but the blood flow is functionally divided into systemic and pulmonary circulations, allowing these animals to change blood volumes, but not pressures, between systemic and pulmonary circulations.

Extensive studies proved not only that the transcription factor Ptx2c plays a crucial role in the differentiation of the myocardium, but also that the initially formed ventricular chamber myocardium has, in its entirety, a trabecular phenotype [45–48]. The early markers of chamber formation Anf and Cx40 remain restricted to the original trabeculated myocardium, and the ventricles develop at the outer curvature of the heart tube, initially forming trabeculated myocardium [45–48].

The hemodynamic significance of these anatomical, echocardiographic, and cardiac MRI findings has to be evaluated by functional dynamic investigations.

Limits of the Study

a) amphibians such as the Xenopus *Laevis* have a single ventricle, both in terms of morphology and function, whereas children with functionally single ventricle typically have two ventricles albeit in a setting of one ventricle being severely hypoplastic.
b) our research project is limited to the phenotyping; however, we used the novel and unique combination, never used before in this setting, of correlating microscopic dissection and photographs with two imaging modalities, echocardiography and cardiac MRI.
c) our observations are the indispensable initial step toward a complete analysis of the function of the frogs heart, by studying the systemic and pulmonary flows distribution with Doppler and ecg-gated MRI. These should provide high quality of innovation and creativity for our translational research.

Conclusion

The findings of our observations confirm the morphological structure of the cardiovascular anatomy of the *Xenopus Laevis*, with atrial situs solitus, double-inlet single ventricle with single trunco-conal outlet, divided in two truncal branches supplying the total body and lung perfusion. The presence of intact inter-atrial septum and helical structure at the outlet of the single ventricle seems designed to allow a favorable streaming between the oxygen saturated and less saturated blood. This could explain why the *Xenopus Laevis* can live many years, despite the presence of a single ventricle. These speculations have to be confirmed by functional studies performed with echocardiography and cardiac MRI.

Acknowledgements We would like to acknowledge Thomas H. Gomez, Mark E. Corkins, Noelia E. Flores, and Jesse C. Whitney, for the great help received for this study in the animal facility at the University of Texas Health McGovern Medical School.

Funding The study did not receive any funding.

Declarations

Conflict of interest The Authors have no disclosure of any conflict of interest, financial and non-financial.

References

1. Corno AF, Becker AE, Bulterijs AHK et al (1982) Univentricular heart: can we alter the natural history? Ann Thorac Surg 34:716–726
2. Marcelletti C, Corno AF, Giannico S, Marino B (1990) Inferior vena cava to pulmonary artery extracardiac conduit: a new form of right heart bypass. J Thorac Cardiovasc Surg 100:228–232
3. Giannico S, Corno AF, Marino B et al (1992) Total extracardiac right heart bypass. Circulation 86:110–117
4. Buchhorn R, Bartmus D, Buhre W, Bursch J (2001) Pathogenetic mechanisms of venous congestion after the Fontan procedure. Cardiol Young 11:161–168
5. Duncan BW, Desai S (2003) Pulmonary arteriovenous malformations after cavopulmonary anastomosis. Ann Thorac Surg 76:1759–1766
6. Narkewicz MR, Sondheimer HM, Ziegler JW (2003) Hepatic dysfunction following the Fontan operation. J Pediatr Gastroenterol Nutr 36:352–357
7. de Leval MR, Deanfield JE (2010) Four decades of Fontan palliation. Nat Rev Cardiol 7:520–527
8. Gewillig M, Brown SC (2016) The Fontan circulation after 45 years: update in physiology. Heart 102:1081–1086
9. Pundi KN, Pundi KN, Johnson JN et al (2017) Sudden cardiac death and late arrhythmias after the Fontan operation. Congenit Heart Dis 12:17–23
10. Dennis M, Zannino D, du Plessis K et al (2018) Clinical outcomes in adolescents and adults after the Fontan procedure. J Am Coll Cardiol 71:1009–1017
11. Claessen G, La Gerche A, Van De Bruaene A et al (2019) Heart rate reserve in Fontan patients: chronotropic incompetence or hemodynamic limitation? J Am Heart Assoc 8:e012008. https://doi.org/10.1161/JAHA.119.012008
12. Restaino G, Dirksen MS, de Roos A (2004) Long-term survival in a case of unoperated single ventricle. Int J Cardiovasc Imaging 20:221–225
13. Ammash NM, Warnes CA (1996) Survival into adulthood of patients with unoperated single ventricle. Am J Cardiol 77:542–544
14. Poterucha JT, Anavekar NS, Egbe AC et al (2016) Survival and outcomes of patients with unoperated single ventricle. Heart 102:216–222
15. Corno AF, Vergara C, Subramanian C et al (2010) Assisted Fontan procedure: animal and in vitro models and computational fluid dynamics study. Interactive CardioVasc Thorac Surg 10:679–684
16. Puelz C, Acosta S, Riviere B, Penny DJ, Brady KM, Rusin CG (2017) A computational study of the Fontan circulation with fenestration or hepatic vein exclusion. Comput Biol Med 89:405–418
17. Rijnberg FM, Hazekamp MG, Wentzel JJ et al (2018) Energetics of blood flow in cardiovascular disease concept and clinical implications of adverse energetics in patients with a Fontan circulation. Circulation 137:2393–2407
18. Hsia TY, Conover T, Figliola R, for the Modeling of Congenital Hearts Alliance (MOCHA) Investigators (2020) Computational modeling to support surgical decision making in single ventricle physiology. Semin Thorac Cardiovasc Surg Pediatr Card Surg Ann 23:2–10
19. Hicks JW (2002) The physiological and evolutionary significance of cardiovascular shunting patterns in reptiles. News Physiol Sci 17:241–245
20. Driedzic WR, Gesser H (1994) Energy metabolism and contractility in ectothermic vertebrate hearts: hypoxia, acidosis and low temperature. Physiol Rev 74:221–258
21. Burggren WW, Warburton S (2007) Amphibians as animal models for laboratory research in physiology. ILAR J 48:260–269
22. O'Rourke DP, Rosenbaum MD (2015). Biology and diseases of amphibians. In: Laboratory animal medicine, third edn. Elsevier Inc, Amsterdam, pp 931–965. https://doi.org/10.1016/B978-0-12-409527-4.00018-3
23. Pokhrel P (2016). Respiratory system in frogs. BiologyOctober 14. https://microbiologynotes.com/respiratory-system-frog/
24. Chambers WN, Criscittiello MG, Goodale F (1961) Cor triloculare biatriatum. Survival to adult life. Circulation 23:91–101
25. Sharma HL (1961) The circulatory mechanism and anatomy of the heart of the frog, *Rana pipiens*. J Morphol 109:323–349
26. Haberich FJ (1965) The functional separation of venous and arterial blood in the univentricular frog heart. Ann N Y Acad Sci 127:459–476
27. Hillman SS, Hedrick MS, Kohl ZF (2014) Net cardiac shunts in anuran amphibians: physiology or physics? J Exp Biol 217:2844–2847
28. Meyer SL, Jongbloed MR, Ho SY et al (2017) Intracardiac anatomical relationships and potential for streaming in double inlet left ventricles. PLosOne. https://doi.org/10.1371/journal.pone.0188048
29. Lagerstrand G, Poupa O (1980) Effects of calcium and pH on the mechanical performance of heart muscle in the frog, *Rana temporaria*, during anoxia and subsequent recovery. Acta Physiol Scand 108:399–404
30. Ventura-Clapier R, Vassort G (1980) Electrical and mechanical activities of frog heart during energetic deficiency. J Muscle Res Cell Motil 1:429–444
31. Knight VA, Richardson DR, Makoba B (1989) Use of frog ventricle to examine mechanical and electrical activity of heart. Am J Physiol 256:S9-13

32. Bartlett HL, Escalera RB, Patel SS et al (2010) Echocardiographic assessment of cardiac morphology and function in *Xenopus*. Comp Med 60:107–113
33. Van Praagh R (1977) Terminology of congenital heart disease: glossary and commentary. Circulation 56:139–143
34. Jensen B, Boukens JD, Postma AV et al (2012) Identifying the evolutionary building block of the cardiac conduction system. PlosOne 7:e44231. https://doi.org/10.1371/journal.pone.0044231
35. Lohr JL, Danos MC, Yost HJ (1977) Left-right asymmetry and a nodal-related gene is regulated by dorsoanterior midline structures during *Xenopus* development. Development 124:1465–1472
36. Levin M, Mercola M (1998) Evolutionary conservation of mechanisms upstream of asymmetric Nodal expression: reconciling chick and *Xenopus*. Develop Genet 23:185–193
37. Lohr JL, Danos MC, Groth TV, Yost HJ (1998) Maintenance of asymmetric Nodal expression in *Xenopus laevis*. Develop Genet 23:194–202
38. Bajolle F, Zaffran S, Kelly RG et al (2006) Rotation of the myocardial wall of the outflow tract is implicated in the normal positioning of the great arteries. Circ Res 94:421–428
39. Grande C, Patel NH (2008) Nodal signalling is involved in left-right asymmetry in snails. Nature 457:1007–1011
40. Oliverio M, Digiglio MC, Versacci P, Dallapiccola B, Marino B (2010) Shells and heart: are human laterality and chirality of snails controlled by the same maternal genes? Am J Med Genet 152:2419–2425
41. Versacci P, Digiglio MC, Oliverio M, Dallapiccola B, Marino B (2011) The heart and shell. Anatomical and genetic similarities. Am Heart J 161:647–649
42. Marino B, Digilio MC, Di Donato R (2002) Transposition of the great arteries in asplenia and polysplenia phenotypes. Am J Med Genet 110:292–294
43. Marino B, Corno AF (2003) Spiral pattern: universe, normal heart, and complex congenital heart defects. J Thorac Cardiovasc Surg 126:1225–1226
44. DeLuca A, Sarkozy A, Consoli F et al (2020) familial transposition of the great arteries caused by multiple mutations in laterality genes. Heart 96:673–677
45. Christoffels VM, Habets PEMH, Franco D et al (2000) Chamber formation and morphogenesis in the developing mammalian heart. Develop Biol 223:266–278
46. Lamers VH, Moorman AFM (2002) Cardiac septation: a late contricution of the embryonic primary myocardium to heart morphogenesis. Circ Res 91:93–103
47. Moorman AFM, Christoffels VM (2003) Cardiac chamber formation: development, genes and evolution. Physiol Rev 83:1223–1267
48. Sylva M, van den Hoff MJB, Moorman AFM (2014) Development of the human heart. Am J Med Genet 164A:1347–1371